Journal of Medicinal Chemistry



Drug Annotation

# Development of a Dual-Acting Antibacterial Agent (TNP-2092) for the Treatment of Persistent Bacterial Infections

Zhenkun Ma, and Anthony Simon Lynch

*J. Med. Chem.*, **Just Accepted Manuscript** • DOI: 10.1021/acs.jmedchem.6b00485 • Publication Date (Web): 23 Jun 2016

# Development of a Dual-Acting Antibacterial Agent (TNP-2092) for the Treatment of Persistent Bacterial Infections

Zhenkun Ma[1*] and Anthony Simon Lynch[2]

[1]TenNor Therapeutics Ltd., 218 Xinghu St. Suzhou Industrial Park, China 215123

[2]Janssen Research & Development LLC., 1400 McKean Road, Spring House, PA 18940, USA.

[*]Corresponding Author

## ABSTRACT

The clinical management of prosthetic joint infections and other persistent bacterial infections represents a major unmet medical need. The rifamycins are one of the most potent antibiotic classes against persistent bacterial infections, but bacteria can develop resistance to rifamycins rapidly and the clinical utility of the rifamycin class is typically limited to antibiotic combinations to minimize the development of resistance. To develop a better therapy against persistent bacterial infections, a series of rifamycin based bi-functional molecules were designed, synthesized and evaluated with the goal to identify a dual-acting drug that maintains the potent activity of rifamycins against persistent pathogens and at the same time minimize the development of rifamycin resistance. TNP-2092 was identified as a drug candidate and is currently in an early-stage of clinical development for the treatment of prosthetic joint infections.

**Keywords:** rifamycin, dual-action, bacterial persistent infections, bacterial biofilms, prosthetic joint infections, antibiotic resistance.

## INTRODUCTION

Prosthetic joint infections (PJIs) are difficult to treat and are often associated with significant morbidity and substantial health care expenditures.[1] The incidence of prosthesis implantations and as a consequence, the burden of PJIs is expected to continue to rise rapidly. In the United States, there were about 1 million total hip and knee replacement surgeries performed in 2010 and this number is projected to reach 4 million by 2030. However, the implementation of enhanced infection prevention measures does not appear to have resulted in a significant reduction in the PJI incident rate in the United States. In fact, the incidence rate has increased slightly from 1.99 to 2.18% for hip and from 2.05 to 2.18% for knee replacement from 2001 to 2009, respectively.[2] The management of PJIs is difficult, requiring surgical intervention accompanied by prolonged antibiotic therapy. For early-stage infections (less than 30 days post-implantation or less than 3 weeks after the onset of infectious symptoms) with a well-fixed prosthesis without a sinus tract, a debridement and prosthesis retention strategy is advised. All other patients should proceed to one-stage or two-stage prosthesis exchange (revision) surgery. For certain patients, exchange surgery is not possible and limb amputation becomes the last resort [3].

*Staphylococcus aure*us and coagulase-negative staphylococci (CoNS) are responsible for the majority of PJIs and are associated with higher treatment failure rates than observed with other causative pathogens. The treatment strategy for staphylococcal PJIs involves a prolonged rifampin-based combination therapy, including 2-6 weeks of intravenous antibiotic therapy in combination with oral rifampin, followed by rifampin plus a companion antibiotic for a total of 3-6 months.[3] The formation of bacterial biofilms on the surface of prosthesis appears to play an important role in the pathogenesis of PJI and is believed to be the underlying mechanism for persistence. It is a well-known phenomenon that pathogens living in bacterial biofilms can effectively evade host immune responses and can become tolerant to antibiotic treatment.[4]

PJIs are devastating to patients and have significant economic impact to the healthcare system. Patient suffering and treatment costs increase dramatically with more invasive surgical intervention strategies. Early diagnosis and early treatment are critical to reduce the need for exchange surgery, permanent resection and amputation. However, the least invasive PJI treatment strategy – debridement and retention procedure can only be applied to patients who have a well-fixed prosthesis without sinus tract involvement and within the first month of prosthesis implantation or within 3 weeks of the onset of infection symptoms. Despite the stringent inclusion criteria and prolonged antibiotic therapy, this treatment strategy can still be associated with low and unreliable treatment outcomes with the overall success rate reported as 14%-100%.[3]

Overall, there is an urgent need for better therapies against persistent bacterial infections associated with bacterial biofilm formation. A new antibacterial agent that is more efficacious in eradicating pathogens living in bacterial biofilms, particularly for those formed by *S. aureus* and CoNS, could represent a major advancement in PJI treatment. Such an agent could potentially lead to improved cure rate, shorter treatment duration and simplified therapy under the current treatment guidelines. More importantly, such an agent could potentially change the PJI treatment paradigm, allowing more patients to utilize the debridement and prosthesis retention treatment strategy and reducing the need for more aggressive surgeries. A more efficacious therapy against bacterial biofilms accompanied by an early diagnostic biomarker for PJI could potentially make a surgery-free PJI treatment strategy a reality.

The rifamycin family of antibiotics is one of the most potent classes known against pathogens living in bacterial biofilms.[5] Rifampin is a member of the rifamycin family and plays an essential role in current staphylococcal PJI management.[6] However, pathogens develop resistance to rifamycins rapidly as single point mutations on bacterial RNA polymerase typically confer high levels of rifamycin resistance. Hence, in clinical practice, rifamycins need always to be used in

combination with other antibiotics in order to minimize resistance development. To take advantage of the potent activity of the rifamycin class against pathogens living in biofilms and at the same time minimizing the emergence of resistance, a new strategy is currently in development by attaching another antibiotic functionality to the rifamycin core to form hybrid antimicrobials with a dual-mechanism of action. In this article we summarize the efforts in discovering and developing dual-action molecule **1** (TNP-2092, CBR-2092) based on rifamycins.

## RIFAMYCINS AS LEADS FOR NEW AGENTS TO TREAT PERSISTENT BACTERIAL INFECTIONS

The rifamycin class of antibiotics was first discovered in 1957 as natural products produced by *Streptomyces mediterranei.*[7] However, the naturally occurring rifamycins are unsuitable as therapeutic agents due to relatively poor potency and undesirable pharmacokinetics. Synthetic modifications of the natural products have led to significant improvements in potency and pharmacokinetic properties. Currently, there are four semi-synthetic compounds, rifampin, rifapentine, rifabutin and rifaximin in clinical use. Rifampin is the cornerstone agent in a four-drug combination regimen for the treatment of tuberculosis.[8] Rifapentine possesses a longer half-life than rifampin and can be used as intermittent therapy for the treatment of tuberculosis. Rifabutin exhibits a reduced cytochrome P450 induction potential and has advantage in treating tuberculosis and human immunodeficiency virus co-infected patients. Rifaximin is unique in its pharmacokinetics; it is not orally absorbable and is used for the treatment of symptoms associated with gastrointestinal tract infections, including travelers' diarrhea, hepatic encephalopathy and irritable bowel syndrome with diarrhea.[9]

The mechanism of action of the rifamycin class has been extensively studied. Rifamycins are DNA-dependent RNA polymerase inhibitors. They bind to the β subunit of the bacterial RNA polymerase in the RNA exit channel and block RNA elongation during the transcription

process.[10] Pathogens develop resistance to rifamycins rapidly mainly due to point mutations in the rifamycin-binding region of the β subunit of the bacterial RNA polymerase. A single point mutation of one of the key residues in the rifamycin binding pocket can lead to high levels of rifamycin resistance.[11]

One of the key characteristics of the rifamycin class is its activity against persistent bacterial infections. Unlike the majority of other antibiotic classes that require active bacterial growth to exert their antibacterial activity, rifamycins are active against pathogens in slow growing, stationary and non-replicating metabolic states, owing to its ability to interfere with the critical bacterial gene transcription process and its ability to distribute to deep-seated infection sites. These unique attributes have important clinical applications and have made rifamycin class agents the drug-of-choice for many persistent bacterial infections. Rifampin is the most important member of the rifamycin class from a clinical perspective and is a key component of the four-drug regimen for the treatment of tuberculosis. Rifampin is mainly responsible for shortening the duration of tuberculosis therapy from 12 months to the current 6 months.[8, 12] Rifampin is also being utilized or studied for the treatment of other persistent and difficult-to-treat bacterial infections including infective endocarditis, osteomyelitis and PJIs. [5, 13]

Rifampin has demonstrated good activity against pathogens living in bacterial biofilms *in vitro* and in animal models of biofilm-associated, persistent infections[5, 14] and is recommended as a key component in the treatment of PJIs according to various clinical practice guidelines.[3, 15] The contribution of rifampin in the management of PJIs has been demonstrated in many clinical trials.[6b, 16] It has been well documented that rifampin should always be used in combinations with other antibiotics to minimize the development of resistance.[17] In addition, the companion antibiotic can help to kill planktonic bacterial and prevent bacteremia. Various antibiotics have been explored as companion agents for rifampin in the management of the early stage of staphylococcal PJIs. The clinical practice guidelines published by the Infectious Diseases

Society of America (IDSA) recommends 2-6 weeks of a pathogen-specific intravenous antimicrobial therapy in combination with rifampin 300-450 mg given orally twice daily followed by rifampin plus a companion oral drug for a total of 3 months for a total hip arthroplasty infection and 6 months for a total knee arthroplasty infection.[3] Recommended oral companion drugs for rifampin are two fluoroquinolones, ciprofloxacin and levofloxacin, based on *in vitro* and *in vivo* animal studies in combination with clinical evidence.[16b]

Currently, the rifampin-containing drug combinations are perhaps the best option available for the treatment of staphylococcal PJIs and associated with improved cure rate. However, the current treatment strategy is clearly inadequate as it requires parallel surgical intervention to be effective and despite this, the success rate is still low and unreliable and the consequence of treatment failure is devastating.

## DESIGN, SYNTHESIS AND EVALUATION OF DUAL-ACTING RIFAMYCINS

One potential approach to improve PJI treatment is through the development of rifamycin based dual-action molecules. This approach takes advantage of the proven efficacy of the rifamycin combinations against PJIs and in the same time to alleviate the problems associated with the use of drug combinations.

There are a number of problems associated with rifampin based drug combinations in the treatment of PJI. First, rifampin and its companion drug may have different pharmacokinetic profiles. For example, they may have different serum half-lives and tissue distributions. This can lead to unbalanced drug exposure at the infection site, leaving rifampin “unprotected” from a resistance-development perspective at certain points in the dosing cycle and therein allowing for the development of rifampin resistance. Second, the antibacterial spectrum of the companion antibiotic (*e.g.,* ciprofloxacin) can be very different from rifampin, and represents another cause for concern for the development of resistance by organisms not fully covered by both antibiotics.

Third, there can be significant additive toxicity associated with the use of drug combinations or other undesired drug-drug interactions that impact the pharmacokinetics of companion agents. Fourth, patients have to take multiple different antibiotics; particularly in the initial phase of the PJI treatment where rifampin is given orally and other drugs are given intravenously. Finally, another specific issue associated with the recommended PJI regimen rifampin plus a fluoroquinolone (ciprofloxacin or levofloxacin) combination is the antagonism between these two agents. The antagonistic effect between rifampin and the fluoroquinolone has been observed *in vitro* and *in vivo* with different members of the fluoroquinolone class and against different pathogens.[18] A dual-acting molecule that contains a rifamycin and a fluoroquinolone structural motif can theoretically address the above problems associated with rifampin and fluoroquinolone drug combinations.

As a general strategy to minimize antibiotic resistance development, dual-acting antibacterial molecules that can attack bacteria with two different modes of action have been explored for many years. This area has been reviewed several times in the past few years, including a comprehensive chemistry review published in 2015.[19] One of the early examples of the dual-acting approach is **2** (Ro 23-9424), a hybrid compound comprised of a cephalosporin and a fluoroquinolone moiety.[20] Compound **2** itself behaves like a cephalosporin and does not possess the mode of action of a fluoroquinolone. However, **2** can be cleaved either chemically or metabolically to release the fleroxacin moiety and this degradation product can then exert its antibacterial activity via the mode of action of a fluoroquinolone (Figure 1). Compound **2** is therefore not a true dual-acting antibacterial agent and is in-effect a cephalosporin acting as a fluoroquinolone pro-drug. However, **2** failed to demonstrate any advantage over a cephalosporin or a fluoroquinolone in preventing resistance development.[21]

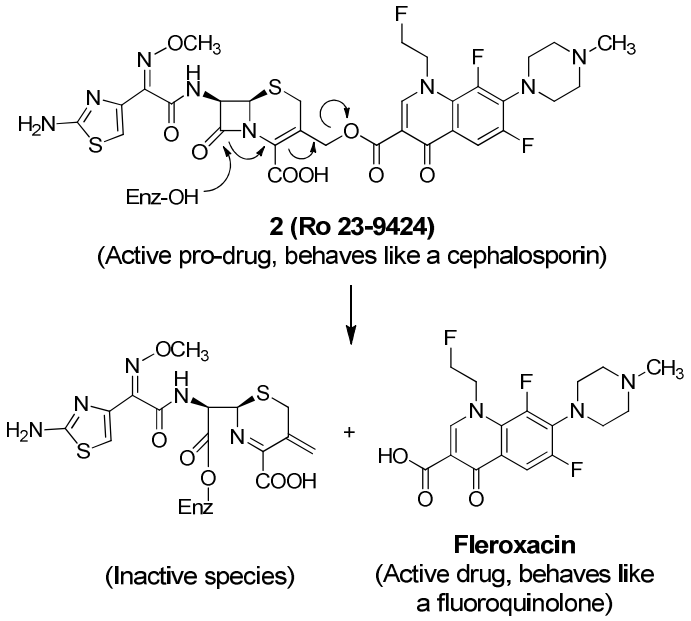


**Figure 1**: Proposed enzymatic activation process for cephalosporin-fluoroquinolone hybrid compound **2**.

More recent efforts have focused on the development of non-cleavable dual-action molecules. Antibiotic classes involved include fluoroquinolones, macrolides, β-lactams, oxazolidinones, tetracyclines, aminoglycosides, rifamycins, glycopeptides and some less known antibiotic classes.[19] One of the non-cleavable antibiotic hybrids is **3 (**cadazolid), formed by a fluoroquinolone and an oxazolidinone core via a stable linker (Figure 2). Compound **3** is currently in Phase III clinical trials for the treatment of *Clostridium difficile* infections. Mode of action studies conducted with *C. diffi*cile indicated that **3** retains the mode of action of an oxazolidinone but failed to demonstrate a substantial contribution from the fluoroquinolone function.[22] In effect, **3** behaves like a more potent linezolid with a low systemic exposure and a high local concentration in the gastrointestinal tract.

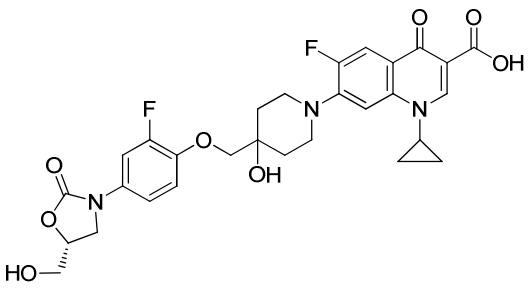

**Figure 2:** Structure of oxazolidinone-fluoroquinolone hybrid compound **3** (Cadazolid).

One of the key components for a successful dual-action antibacterial program is to implement a robust compound evaluation strategy. An experienced medicinal chemist with knowledge of the structure-activity relationships for each of the parent antibiotic classes can design and synthesize certain hybrid compounds containing two antibiotic motifs. However, the resulting hybrid compounds may or may not have the desired dual modes of action. Critical data need to be generated rapidly to guide the lead optimization and candidate selection process. A robust compound evaluation strategy should include assays to progressively assess compounds in enzyme, whole-cell and animal levels. Such an evaluation scheme is shown in Figure 3 which includes (i) validated biochemical assays to assess the activity and potency of the hybrid compounds against target proteins/enzymes of both parent drugs, (ii) whole cell assays on isogenic bacterial panels with defined antibiotic resistance mutations on drug targets associated with both parent drugs, and (iii) validated animal models of the target disease indication(s).

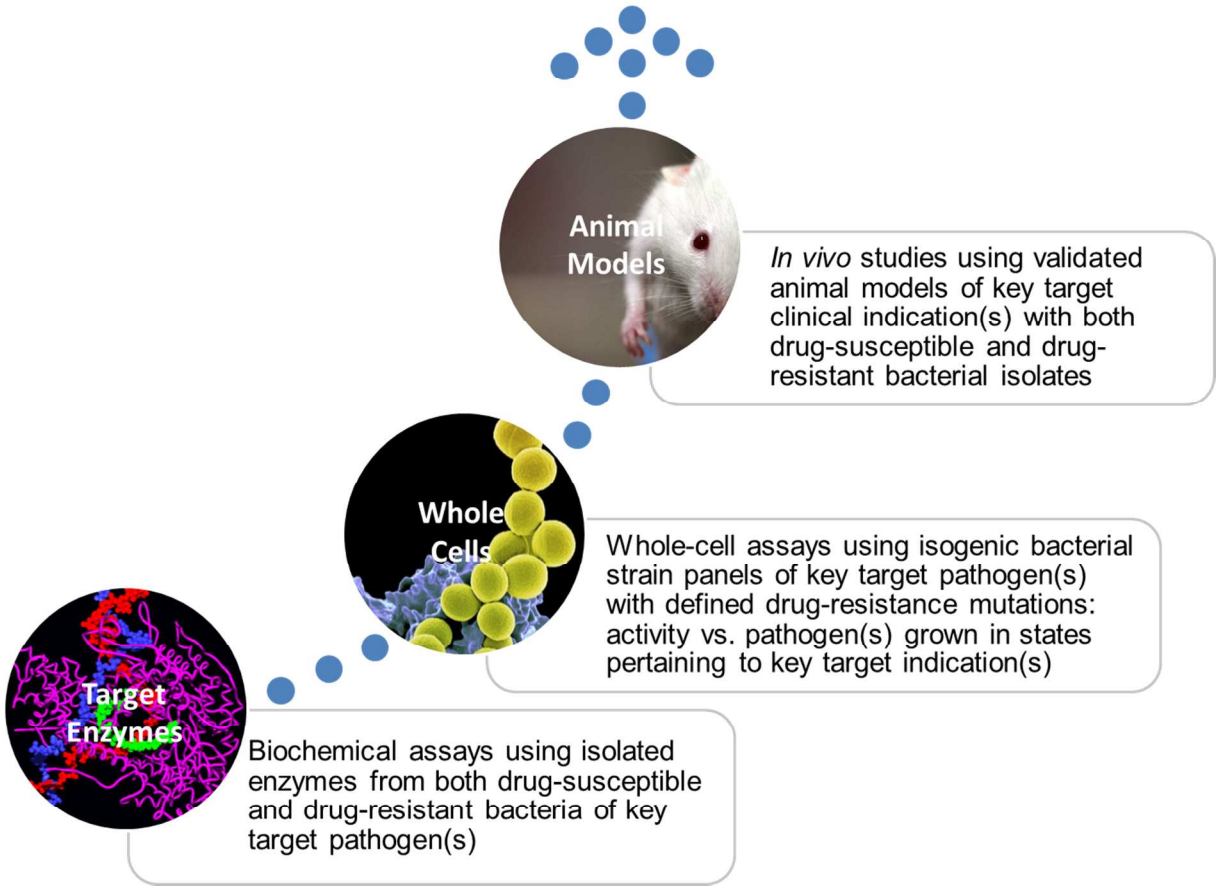


**Figure 3:** Biological evaluation strategy for a dual-action antimicrobial program.

Rifamycins are a well-studied class of antibiotics with an extensive knowledge of structure-activity relationships pertaining to *in vitro* and *in vivo* activity accumulated over the past 50 years. Recently, the details of the interaction between rifampin and its drug target, bacterial RNA polymerase, have been elucidated by high-resolution crystallization studies of the *Thermus aquaticus* core enzyme in complex with rifampin.[10] Both crystal structural interactions between rifampin and RNA polymerase and structure-activity relationships suggest that the groups attached to the C-3 and C-25 positions of rifampin are pointing to open space and can therefore be explored as sites for attaching a secondary antibiotic group [Figure 4].

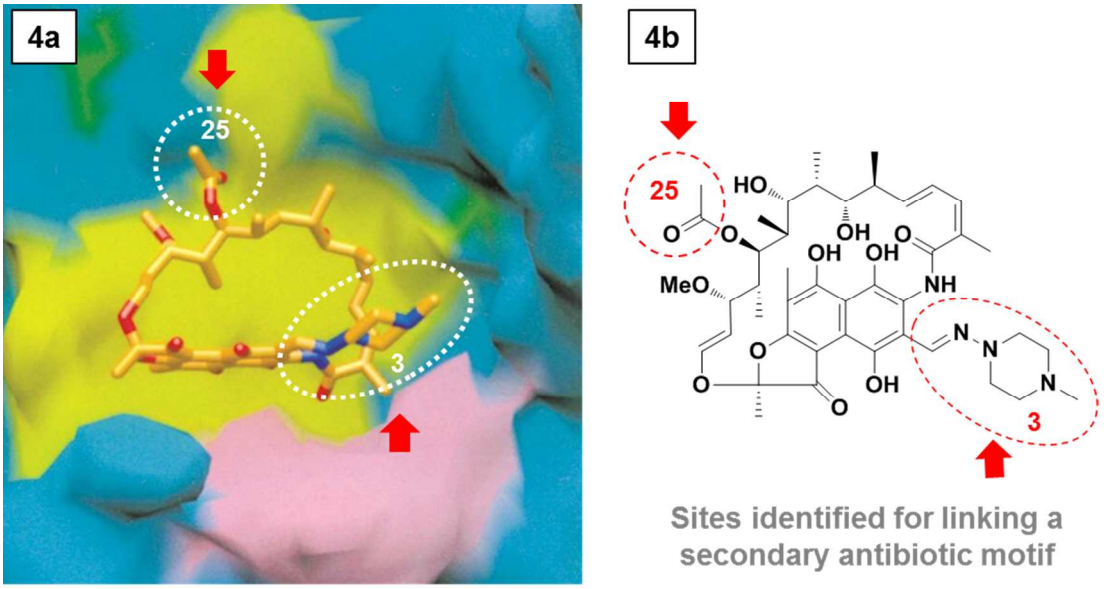


**Figure 4:** Structural interactions between rifampin and RNA polymerase (4a) and structure-activity relationships (4b) suggest that the groups attached to the C-3 and C-25 positions of the rifamycin scaffold are pointing to open space and can be explored for attaching a secondary antibiotic motif. (Image 4a reprinted and modified from Cell, Vol. 104, Campbell EA, Korzheva N, Mustaev A, Murakami K, Nair S, Goldfarb A, Darst SA, Structural mechanism for rifampicin inhibition of bacterial RNA polymerase, Page 901-912, Copyright 2001, with permission from Elsevier).

The majority of rifamycin-based hybrid antibiotic compounds prepared to date utilize the C-3 position as the linking point. In addition to accessing an open space from the rifamycin scaffold docked into its binding site on RNA polymerase, the C-3 position is chemically versatile which can be easily functionalized to introduce various groups serving as linkers.[23] The C-3 position together with its adjacent C-4 position can also form a new heterocycle that in turn can serve as the linking point for a secondary antibiotic.[24] The carbonyl group at the C-11 position can be functionalized via an oxime group and serve as the linking point for a secondary antibiotic to access the same open space as that of the C-3 position.[25] The acetyl group at the C-25 position

can be replaced with a carbamate group and serve as a linking point for further derivatization.[26] The positions on rifamycin that have been explored as linking points and the chemistry strategies utilized to link a secondary antibiotic functionality are summarized in Figure 5.

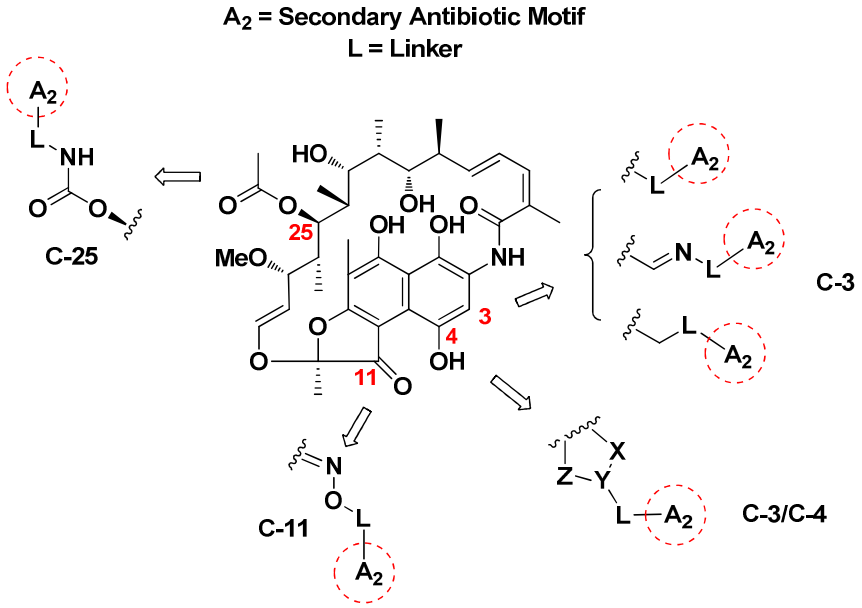


**Figure 5:** Positions on the rifamycin scaffold and strategies that have been utilized for linking a secondary antibiotic group.

The selection of the secondary antibiotic is important. From a mechanistic standpoint, the secondary antibiotic should be active against the target pathogen(s) that the resulting dual-acting compound is intended to treat and it should not have cross-resistance with the primary antibiotic. In addition, it should possess a well-defined structure-activity relationship and/or high resolution co-crystal structural information allowing for the rapid assembly of hybrid molecules with dual mechanisms of action. Several antibiotic classes have been explored as matching partners for developing dual-acting rifamycins to date. They include quinolones (including non-fluoroquinolones, fluoroquinolones and their bioisostere quinolizinones)[23, 25b, 25c, 27], macrolides (including 14-, 15- and 16-membered ring macrolides)[28], oxazolidinones[28] and nitroimidazoles.[24c] *In vitro* minimum inhibitory concentration (MIC) data published in the cited

patent literature indicate that these hybrid series are active against rifamycin-susceptible and resistant bacterial strains – an indicator of genuine dual-action.

## OPTIMIZATION AND DEVELOPMENT OF RIFAMYCIN-QUINOLONE DUAL-ACTING ANTIMICROBIALS

Rifamycin-quinolone hybrid compounds have been studied the most extensively among those rifamycin-based hybrid series. A variety of quinolone core structures as depicted in Figure 6 have been explored as the matching partners for rifamycin.[23, 25a, 25c, 27] These quinolone core structures are associated with various fluoroquinolone, non-fluoroquinolone and quinolizinone sub-classes. Quinolizinones (also known as 2-pyridones) are close analogs of quinolones where the N-1 nitrogen atom is switched with the C-5 carbon atom to produce a family of highly active bioisosteres.[29] Quinolizinones, exemplified by **4 (**ABT-719), are potent and balanced inhibitors of bacterial DNA gyrase and topoisomerase IV and exhibit potent antibacterial activities against both Gram-positive and Gram-negative pathogens.[29-30] However, no quinolizinone class of antibacterial agents has been commercialized to date. The positions on the rifamycin scaffold that have been utilized for attaching the quinolone structures are C-3, C-3/C-4, C-11 and C-25 using the strategy discussed previously (Figure 5). The structures for the linker group vary widely based on published patent literature and appear to have significant impact on the antibacterial activity of the hybrid compounds. However, the detailed structure-activity relationships around the rifamycin-quinolone series have yet to be reported.

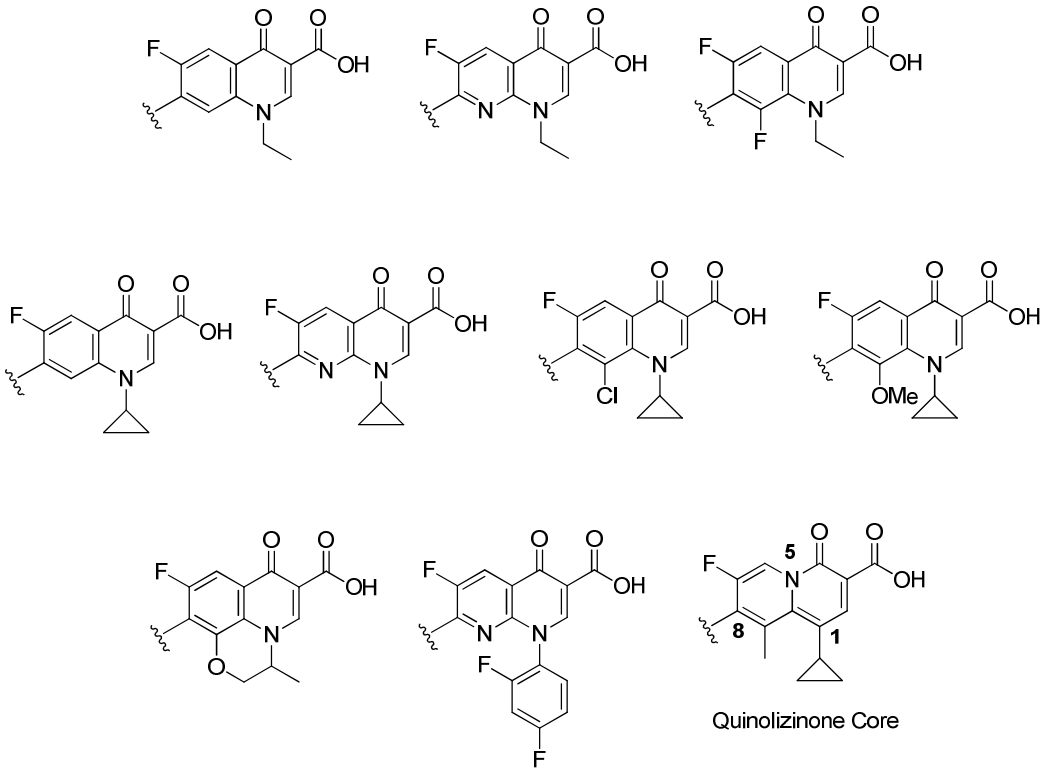


**Figure 6:** Quinolone core structures that have been explored as matching partners for rifamycins.

Compound **1** is the leading molecule from the rifamycin-quinolone hybrid series currently in clinical development.[31] The compound is formed by a rifamycin and a quinolizinone core connected via the C-3 position from the rifamycin side and the C-8 position from the quinolizinone side. The linker group resembles the structural characteristics of the side chains of rifampin and **4** joined together covalently (Figure 7).

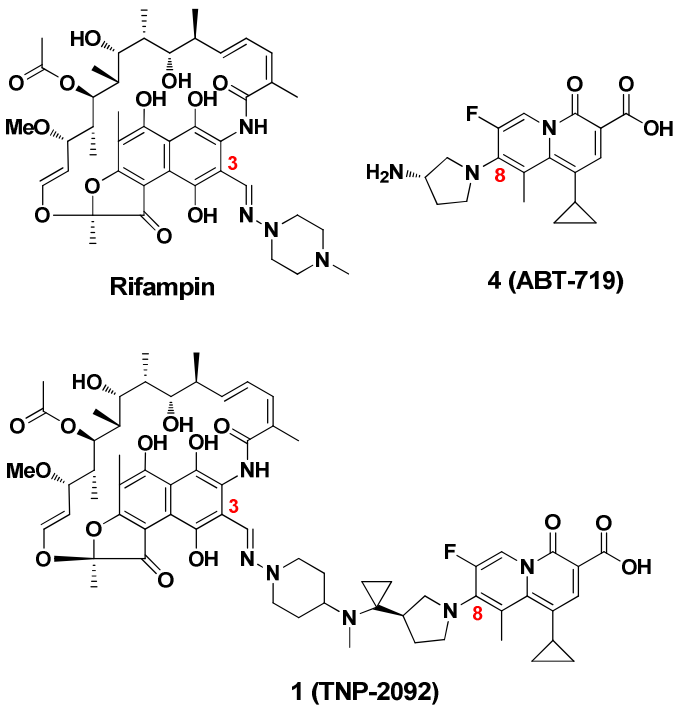


**Figure 7:** Structure of rifampin, quinolizinone **4** and dual-acting molecule **1**.

Compound **1** was synthesized by connecting the rifamycin core (**14**), quinolizinone core (**11**) and linker group (**10**) together (Scheme 1).[23] Starting from commercially available (*S*)-1-benzyl-3-hydroxypyrrolidine, linker group **10** was prepared in 5 steps. 8-Chloro-1-cyclopropyl-7-fluoro-9-methyl-4-oxo-4H-quinolizinone-3-carboxylate (**11**) was prepared according to published procedures.[29] Coupling of **10** and **11** provided compound **12**. Hydrolysis of the ethyl ester and deprotection of the amine protecting group, provided compound **13**. Finally, **13** was attached to the rifamycin core by first converting the piperidine amino group to a hydrazine, followed by coupling with 3-formalrifamycin (**14**). Compound **1** has been manufactured in kilogram quantities in a similar fashion for multiple times. The synthesis of **1** is illustrated in the experimental session.

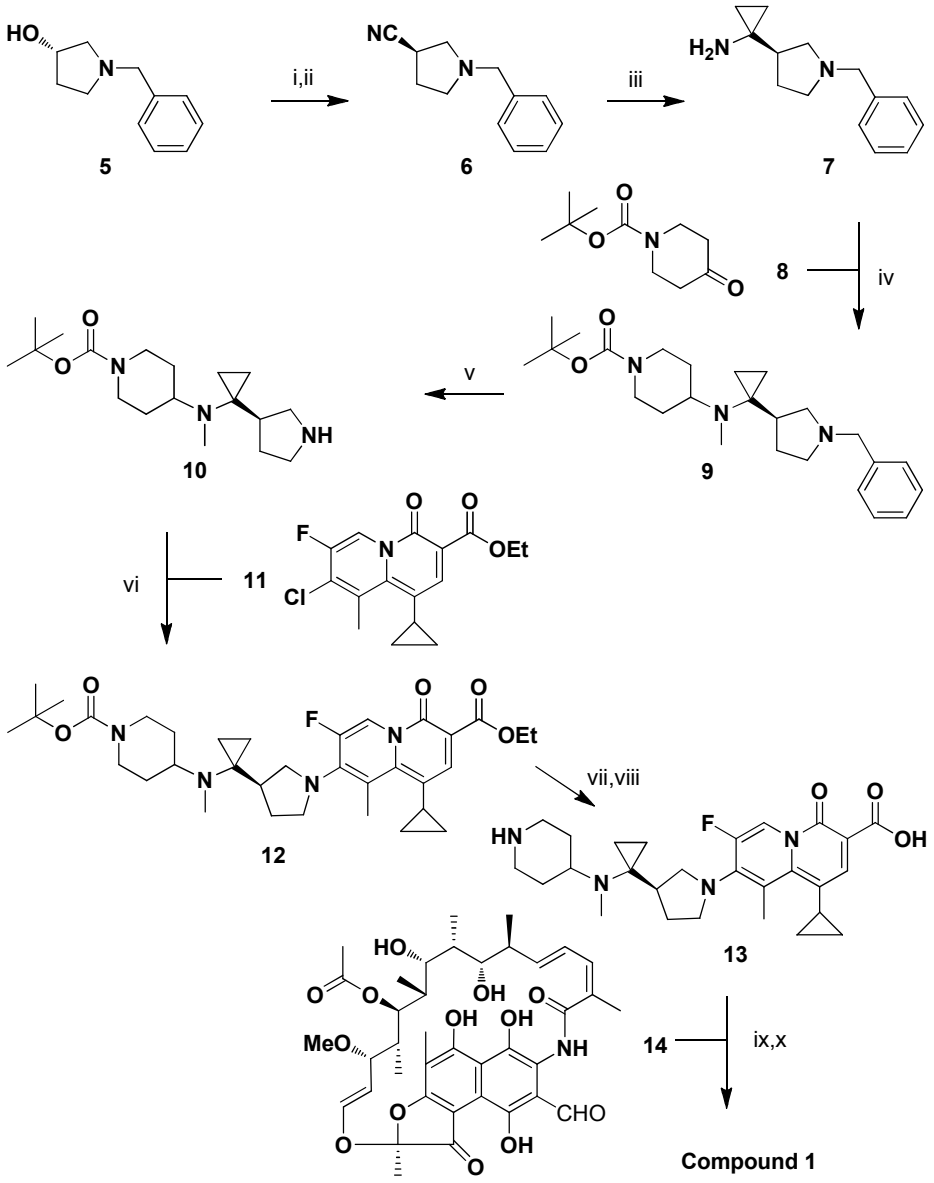


**Scheme 1**: Synthesis of dual-acting molecule **1**.

Reagents and conditions: (i) MsCl, $Et_3N$, toluene, 0°C, 2h; (ii) $Bu_4N^+CN^-$, $CH_3CN$, 65°C, 16h; (iii) $Ti(O\text{-}iPr)_4$, EtMgBr, $Et_2O$/THF, -78°C, 29 min; warm to rt, $BF_3$•$Et_2O$, 2h; (iv) **8**, THF/AcOH, rt, 1 h, then $NaBH(OAc)_3$, rt, overnight; (v) H2, Pd/C, AcOH, 60 psi, rt, 18 h; (vi) **11**, $NaHCO_3$, $CH_3CN$, reflux, 5h; (vii) LiOH, EtOH, 60°C, 1h; (viii) $CF_3CO_2H$, $CH_2Cl_2$, 0°C - rt, 1h; (ix) NaOH, $H_2N\text{-}OSO_3H$, 0°C, 1h; (x) 3-formal rifamycin (**14**), MeOH/THF, rt, 30 min.

## PRECLINICAL CHARACTERIZATION

Preclinical studies of the *in vitro* and *in vivo* activities of **1** were described in a series of posters presented at the 47th (2007) Interscience Conference on Antimicrobial Agents and Chemotherapy[32] and in two subsequent publications.[31]

As is shown in Table 1, biochemical studies using *S. aureus* enzymes indicate that **1** retains rifampin-like potency as an inhibitor of RNA Polymerase (RNAP) and exhibits balanced (equipotent) activity against DNA gyrase and DNA topoisomerase IV (Topo IV) while retaining activity against a common quinolone-resistant (FQ-R) variant (ParC$^{S80F}$) of DNA topoisomerase IV.[32a] No inhibition of human topoisomerase II-alpha (Top2a) by **1** was observed. As is shown in Table 2, minimum inhibitory concentration (MIC) values determined for otherwise isogenic strains of *S. aureus* ATCC 29213 bearing rifamycin (*rpoB*$^{H481Y}$) and/or quinolone (*parC*$^{S80F}$ and *gyrA*$^{S84L}$) resistance alleles confirm that **1** retains rifampin-like potency against quinolone-resistant strains and gatifloxacin-like potency against rifampin-resistant strains. Again, these data support the notion that **1** exhibits antimicrobial activity via combined contributions from both the rifamycin and quinolizinone functions and are consistent with triple targeting of RNA polymerase, DNA gyrase and DNA topoisomerase IV. A serial stepwise passage resistance study conducted with **1** over a period of 26 days yielded a terminal isolate with broth and agar MICs of >16 and 4 μg/mL, respectively, that possessed five target mutations (*rpoB*$^{R484H}$, *gyrA*$^{\Delta L520,\ S84L}$, *parC*$^{<R236>,\ H103Y}$) but was unaltered in efflux properties. Data from time-kill and metabolic labeling experiments also support the notion that the primary activity of **1** in *S. aureus* is driven by its rifamycin function and that activity against rifamycin-resistant strains is mediated by the quinolizinone function. In metabolic labeling experiments, **1** has a primary effect on *de novo* RNA synthesis with delayed, secondary effects on DNA, protein and cell wall synthesis. The more pronounced effect of **1** on DNA synthesis than that observed with rifampin

presumably reflects the secondary mode of action conferred by the quinolizinone part of the molecule.

**Table 1.** Biochemical characterization of **1** and comparators.

| Compound | $IC_{50}$ (μM)[1] | | $CC_{50}$ (μM)[2] | | | | |
|---|---|---|---|---|---|---|---|
| | RNAP (Wild Type) | RNAP (Rif-R, $RpoB^{H481Y}$) | Topo IV (Wild Type) | Gyrase (Wild Type) | Topo IV (FQ-R, $ParC^{S80F}$) | Gyrase (FQ-R, $GyrA^{S84L}$) | Human Topo2a |
| Compound **1** | 0.034 | >25 | 1.7 | 1.5 | 2.7 | >150 | >150 |
| Rifampin | 0.015 | >25 | - | - | - | - | - |
| Ciprofloxacin | - | - | 0.4 | 5 | 31 | >150 | >150 |
| Gatifloxacin | - | - | 0.2 | 0.7 | 13 | 18 | >150 |

[1]The minimum concentration necessary to inhibit 50% ($IC_{50}$) of the RNA product formed in the absence of test agents; [2]Minimum concentration necessary to induce 50% cleavage of a covalently closed DNA substrate ($CC_{50}$).

**Table 2**. Antibacterial activity of **1** and comparator agents against isogenic *Staphylococcus aureus* strains bearing rifamycin and/or quinolone resistance mutations.

| Compound | *Staphylococcus aureus* isogenic strain panel MIC (μg/mL) | | | | | | | |
|---|---|---|---|---|---|---|---|---|
| | Wild Type | *$gyrA^{S84L}$* | *$parC^{S80F}$* | *$gyrA^{S84L}$ $parC^{S80F}$* | *$rpoB^{H481Y}$* | *$rpoB^{H481Y}$ $gyrA^{S84L}$* | *$rpoB^{H481Y}$ $parC^{S80F}$* | *$rpoB^{H481Y}$ $gyrA^{S84L}$ $parC^{S80F}$* |
| **1** (agar) | 0.008 | 0.008 | 0.008 | 0.008 | 0.06 | 0.12 | 0.06 | 0.25 |

| | | | | | | | | |
|---|---|---|---|---|---|---|---|---|
| **1** (broth) | 0.015 | 0.015 | 0.015 | 0.015 | 0.12 | 0.50 | 0.25 | 2 |
| Rifampin | 0.008 | 0.008 | 0.008 | 0.008 | > 250 | > 250 | > 250 | > 250 |
| Ciprofloxacin | 0.25 | 0.25 | 2 | 16 | 0.25 | 0.25 | 2 | 16 |
| Levofloxacin | 0.25 | 0.25 | 1 | 8 | 0.25 | 0.25 | 1 | 8 |
| Gatifloxacin | 0.06 | 0.12 | 0.25 | 8 | 0.06 | 0.12 | 0.25 | 8 |

Table 3 lists the *in vitro* antimicrobial activity of **1** against 175 staphylococci and 125 streptococci compared to those determined in parallel for rifampin and ciprofloxacin. The broth microdilution MICs at which 90% of methicillin-susceptible or methicillin-resistant *S. aureus* (MSSA, MRSA) or *S. epidermidis* (MSSE, MRSE) isolates are inhibited ($MIC_{90}$) by **1** are 0.015, 0.015, 0.008, and 0.5 μg/mL, respectively. The activity of **1** against MSSA, MRSA and MSSE was equivalent to rifampin and improved over ciprofloxacin, whereas **1** was improved over both rifampin and ciprofloxacin against MRSE. $MIC_{90}$ values for **1** against *S. pyogenes*, *S. agalactiae* and *S. pneumoniae* were 0.12, 0.25, and 0.12 μg/mL, respectively and again, equivalent to rifampin and improved over ciprofloxacin.[31b, 32c]

**Table 3.** Antibacterial activities of **1** against clinical isolates of gram-positive bacteria.

| Organism (n) | Compound | MIC (μg/mL)[1] | | |
|---|---|---|---|---|
| | | Range | 50% | 90% |
| *S. aureus* | | | | |
| MSSA (51)[2] | **1** | ≤0.004 - 0.03 | 0.008 | 0.015 |
| | Rifampin | ≤0.008 - 0.06 | 0.015 | 0.015 |
| | Ciprofloxacin | 0.06 - > 4 | 0.25 | 1 |
| MRSA (54)[2] | **1** | ≤ 0.004 - 2 | 0.015 | 0.015 |

| | | | | |
|---|---|---|---|---|
| | Rifampin | ≤ 0.008 - > 4 | 0.015 | 0.015 |
| | Ciprofloxacin | 0.12 - > 4 | > 4 | > 4 |
| *S. epidermidis* | | | | |
| MSSE (35)[2] | **1** | ≤ 0.004 - 0.015 | ≤ 0.008 | 0.008 |
| | Rifampin | ≤ 0.004 - 0.06 | 0.015 | 0.015 |
| | Ciprofloxacin | 0.12 - > 4 | 0.25 | > 4 |
| MRSE (35)[2] | **1** | ≤ 0.004 - 1 | 0.008 | 0.5 |
| | Rifampin | ≤ 0.004 - > 4 | 0.015 | > 4 |
| | Ciprofloxacin | 0.12 - > 4 | > 4 | > 4 |
| *S. pyogenes* (35)[3] | **1** | 0.008 - 0.12 | 0.03 | 0.12 |
| | Rifampin | ≤ 0.008 - 0.25 | 0.06 | 0.12 |
| | Ciprofloxacin | 0.12 - 2 | 0.5 | 1 |
| *S. agalactiae* (35)[3] | **1** | 0.06 - 2 | 0.12 | 0.25 |
| | Rifampin | 0.03 - 2 | 0.12 | 0.12 |
| | Ciprofloxacin | 0.25 - 1 | 0.5 | 1 |
| *S. pneumoniae* (55)[3] | **1** | 0.06 - 0.25 | 0.12 | 0.12 |
| | Rifampin | 0.12 -1 | 0.25 | 0.25 |
| | Ciprofloxacin | 0.5 - > 4 | 2 | > 4 |

[1]Broth microdilution method; [2]Tested in MHII broth with 0.002 % (vol:vol) polysorbate-80; [3]Tested in MHII broth with 5% (vol:vol) LHB and 0.002 % (vol:vol) polysorbate-80.

Compound **1** also exhibited prolonged post-antibiotic and sub-MIC effects in *S. aureus* and are indicative of efficient intracellular uptake and retention. In time-kill studies, **1** exhibited bactericidal activity against both staphylococci and streptococci with rapid, quinolone-like killing of rifampin-resistant strains observed. In spontaneous resistance studies, **1** exhibited activity consistent with balanced contributions from its composite parent antibiotics with a mutant prevention concentration (MPC) of 0.12 μg/mL and a resistance frequency of $<10^{-12}$ determined at 1μg/mL in agar for *S. aureus* ATCC 29213. Finally, in studies of the killing of *S. aureus* residing intracellularly in murine macrophage cells, **1** exhibited prolonged bactericidal activity.[31, 32c, 32d]

The comparative *in vitro* activity of **1** and rifampin+quinolone combinations was assessed using a series of checkerboard assays with fractional inhibitory concentration (FIC) indices determined by the broth microdilution method, time-kill studies, biofilm killing assays and through determination of MPCs.[32b] Antagonism of the rapid killing of *S. aureus* by quinolones in the presence of rifampin was apparent in checkerboard assays via minimal bactericidal concentration (MBC) endpoints and in high density time-kill assays. In the latter, a rifampin+ciprofloxacin combination (1+0.25 μg/mL) is bacteriostatic (< 99.9% kill at 24h) against *S. aureus* ATCC 29213 and resulted in the outgrowth of rifampin-resistant isolates. In contrast, **1** was observed to be bactericidal (≥ 99.9% kill at 24h at 0.25 μg/mL) without the emergence of rifampin resistance. Also in contrast to tested rifampin+quinolone cocktails, **1** promoted eradication of colony biofilms formed by *S. aureus* MSSA or MRSA isolates and exhibited bactericidal activity (>99% kill at 24h at 4 μg/mL) that is greater than that of rifampin+moxifloxacin (≤ 99 % kill at 4+4 μg/mL) combination in killing *S. aureus* cells within murine macrophages.

In further *in vitro* studies, **1** was found to exhibit anti-biofilm activity in a number of alternate assays and retains potent bactericidal activity against staphylococcal cells in the biofilm state.

[32d] In contrast to existing rifamycin class agents, resistance development in biofilm populations was not observed with **1**. These studies hold promise for the potential of **1** in the treatment of biofilm-associated infections.

Pharmacokinetic (PK) properties of **1** were determined following intravenous (IV) administration to mice, rats, rabbits and dogs and indicated a plasma $T_{1/2}$ of 0.4 to 4.1 h in mice, rats and rabbits and 1.6 to 11.7 h in dogs.[32f] The calculated volume of distribution of **1** ranged from 0.08 to 0.52 and 0.09 to 0.17 L/kg in rodents/rabbits and dogs, respectively. Plasma clearance ranged from 0.07 to 0.36 and 0.01 to 0.08 L/h/kg in rodents/rabbits and dogs, respectively. Calculated AUC and $C_{max}$ values were dose proportional for all species. Data from the neutropenic thigh infection model and the drip flow biofilm reactor identified the 24h AUC/MIC ratio as the PD index best correlated with efficacy. [32f]

The *in vivo* efficacy of **1** was determined in various rodent models of staphylococcal and streptococcal infections including acute systemic infections and chronic biofilm-associated infections of indwelling medical devices.[32e] In a mouse septicemia model, $ED_{50}$ values for **1** ranged from 1.4 to 3.8 mg/kg for MSSA, MRSA and FQ-resistant *S. aureus* and 4.8 to 10.7 mg/kg for *S. epidermidis* and *S. pyogenes* infections. In a mouse skin abscess model, **1** exhibited efficacy comparable to rifampin or comparators used to treat complicated skin and skin structure infections (cSSSIs) with $\log_{10}$ CFU reductions of >3.1 to 5.3 observed for MRSA, *S. epidermidis* or *S. pyogenes*. In the rat central venous catheter (CVC) infection model, **1** exhibited equivalent efficacy to rifampin, but significantly improved over cSSSI comparator agents with $\log_{10}$ CFU reductions of 2.8 to 3.4 observed for MSSA and FQ-resistant *S. aureus*. Compound **1** showed effective penetration into granuloma pouch fluid and reduced *S. aureus* counts by 1 to 3.4 $\log_{10}$ CFU after single IV doses of 5 to 25 mg/kg. In the mouse subcutaneous catheter implant model, **1** was more efficacious than rifampin and cSSSI comparators achieving $\log_{10}$ CFU reductions of 5.03, 3.98 and 2.51 against susceptible, FQ-resistant and rifampin-

resistant *S. aureus* isolates, respectively. In addition, **1** exhibited continued suppression of the catheter-localized biofilm infections after therapy was withdrawn.

The *in vivo* efficacy of **1** was further investigated in a rabbit model of infective endocarditis (IE) mediated by MRSA.[32g, 32h] In these studies, rabbit IE was induced with MRSA strain 67-0, following transcarotid-transaortic valve indwelling catheterization. At 24h post-infection, animals received either (i) no therapy (control), (ii) **1** at 10, 25 or 40 mg/kg, iv, bid or (iii) vancomycin at 15 mg/kg, iv, bid. All treatments were for 3 days and 24h after the last dose, target tissues were quantitatively cultured; relapse of infection was also investigated 3d after treatment was discontinued. MICs/MBCs of **1** and vancomycin for MRSA 67-0 were 0.008/0.5 mg/mL, and 1/1 mg/mL, respectively. In these studies, all regimens significantly decreased MRSA densities vs. controls with **1** at 25 and 40 mg/kg exhibiting the greatest efficacy and also prevented relapse. In contrast to vancomycin, sterile tissue cultures were observed in vegetations, kidneys and spleens for all **1** treatment groups following the relapse period with no resistance development to **1** observed.

The comparative efficacy of **1** and rifampin+quinolone combinations was also determined in the rabbit IE model including studies of a quinolone-resistant variant of MRSA 67-0 (QMRSA) bearing both *norA*$^{up}$ (efflux) and DNA topoisomerase IV (*parC*$^{S80F}$) mutations.[32h] At 24h post-infection, animals received either (i) no therapy (control), (ii) **1** 40 mg/kg, iv, bid, ciprofloxacin 20 mg/kg, iv, tid + rifampin 10 mg/kg, im, bid or (iii) levofloxacin 20 mg/kg, iv, bid + rifampin 10 mg/kg, im, bid, all for 3 days. At 24h post-dose, target tissues were cultured. Relapse of infection was investigated 3d after treatment was discontinued. MICs/MBCs of **1**, ciprofloxacin, levofloxacin and rifampin were 0.008/0.5, 16/16, 2/2 and 0.008/2 mg/mL, respectively. Compound **1** significantly reduced QMRSA densities in all target tissues at the end of therapy and relapse. Levofloxacin+rifampin significantly reduced densities but to a lower extent than observed with **1** and ciprofloxacin+rifampin exhibited the lowest overall efficacy.

## SUMMARY AND FUTURE PERSPECTIVES

The development of rifamycin based dual-acting antibacterial agents represents a promising strategy for the treatment of persistent bacterial infections such as PJIs. The dual-action approach could potentially address several major issues associated with the use of rifamycin drug combinations and therefore provide a better therapeutic solution in treating persistent bacterial infections where the standard-of-care requires a rifamycin combination therapy.

The dual-action molecule **1** has demonstrated advantages over rifampin and fluoroquinolone combinations in several aspects. First, it possesses potent and balanced activity against three cellular targets RNA polymerase, DNA gyrase and topoisomerase IV in *S. aureus* and CoNS.[31] Second, it is not a substrate of fluoroquinolone efflux systems and has a low propensity for resistance development. Third, **1** exhibits potent activity against drug resistant pathogens including those resistant to one or both parent drugs and demonstrates better efficacy and resistance development profile than rifamycin+fluoroquinolone combinations in both *in vitro* and *in vivo* biofilm models. Fourth, **1** appears able to alleviate certain safety concerns associated with its parent antibiotic classes such as CYP3A4 induction and hERG inhibition. In completed human Phase I single and multiple ascending dose clinical trials of an intravenous formulation, **1** demonstrates good pharmacokinetic and safety profiles supporting further clinical development for the treatment of PJIs and other persistent bacterial infections.

One of the unexpected observations during the development of rifamycin based dual-action compounds such as **1** is that such dual-action molecules exhibit synergistic effects *in vitro* and *in vivo* improved over the simple parent drug combinations. Such synergies are apparent with several dual-action classes and may represent a general benefit of the dual-action approach. The source and mechanism for such synergy is unclear at this time and represents a direction

of ongoing research for rifamycin-quinolone hybrid agents. Understanding the mechanisms of this synergistic effect may help to design better dual-acting molecules in the future.

The spectrum of the antibacterial activity of a dual-acting molecule can be very different from its parental antibiotics. RNA polymerase and DNA gyrase/topoisomerase IV, the respective drug targets for rifamycins and fluoroquinolones, are essential enzymes in all pathogens. The spectrums of activity for rifamycins and fluoroquinolones are largely a reflection of their ability to reach their intracellular targets. Rifamycins are mainly active against Gram-positive pathogens with difficulties to penetrate the outer cell membrane of Gram-negative organisms, while fluoroquinolones are broad spectrum and active against both Gram-positive and Gram-negative pathogens. The dual-action hybrid molecule **1** is mainly active against Gram-positive pathogens with a spectrum similar to rifampin. However, **1** also demonstrates a better activity than rifampin against certain Gram-negative bacteria such as *Escherichia coli* and *Acinetobacter baumannii*, indicating that **1** may have improved membrane permeability and/or be able to avoid the native efflux systems of these organisms.

A dual-action molecule generally possesses very different absorption, distribution, metabolism and excretion (ADME) properties from its parental antibiotics and its clinical application should be optimized based on its ADME characteristics. Indeed, dual-action molecules such as **1** typically have high molecular weights and exhibit low oral bioavailability and therefore may not be suitable for the development of oral dosage formulations for systemic delivery. However, this low oral absorption could become an advantage for the treatment of diseases associated with gastrointestinal tract infections and this strategy is currently being actively pursued in clinical trials for indications associated with gastrointestinal tract infections.

## EXPERIMENTAL SECTION

Compound **1** has been synthesized many times from milligram to kilogram quantities. The following procedure reproduced from a patent publication is a representation of the process used for large quantity manufacturing of **1**.[23] All starting materials used are either purchased from commercial sources or prepared according to published procedures. Operations involving moisture and/or oxygen sensitive materials are conducted under an atmosphere of nitrogen. Flash chromatography is performed using silica gel 60 as normal phase adsorbent or C18 silica gel as reverse phase adsorbent. Thin layer chromatography (TLC) and preparative thin layer chromatography (PTLC) are performed using pre-coated plates purchased from E. Merck and spots are visualized with ultraviolet light followed by an appropriate staining reagent. Nuclear magnetic resonance (NMR) spectra are recorded on a Varian 400 MHz magnetic resonance spectrometer. $^1$H NMR chemical shift are given in parts-per million (δ) downfield from TMS using the residual solvent signal ($CHCl_3$ =δ 7.27, $CH_3OH$ =δ 3.31) as internal standard. $^1$H NMR information is tabulated in the following format: number of protons, multiplicity (s, singlet; d, doublet; t, triplet; q, quartet; m, multiplet; td, triplet of doublet; dt, doublet of triplet), coupling constant (s) (*J*) in hertz. The prefix *app* is occasionally applied in cases where the true signal multiplicity is unresolved and prefix *br* indicates a broad signal. Electro-spray ionization mass spectra are recorded on a Finnegan LCQ advantage spectrometer. High-performance liquid chromatography (HPLC) analysis for the final compound is performed on Agilent 1100 instrument using a Waters Xterra RP18 column (5 mc-m, 4.6 x 250 mm) and gradient elution (solvent A: 20 mM $NaH_2PO_4$/acetonitrile, 60:40 v/v; solvent B: acetonitrile). HPLC purities for the final compound are ≥95%.

**Synthesis of (*S*)-Methanesulfonic acid 1-benzyl-pyrrolidin-3-yl ester (A)**

(*S*)-1-Benzyl-3-hydroxypyrrolidine (**5**, 20.2 g, 114 mmol) was dissolved in toluene (200 mL). To this stirred solution, triethylamine (20 mL, 142 mmol) was added followed by methanesulfonyl chloride (10.5 mL, 136 mmol) during a period of 40 min at 0ºC. The resultant slurry was allowed

to stir for two hours at 0°C and 7% sodium bicarbonate (200mL) was then added to the reaction mixture. The organic layer was then separated and the aqueous layer extracted with toluene (3x100 mL). The combined organic layers were washed with saturated sodium bicarbonate (3x200 mL), dried over $Na_2SO_4$ and concentrated under reduced pressure to give (*S*)-methanesulfonic acid 1-benzyl-pyrrolidin-3-yl ester as a yellow oil (28 g, 96%). The material was used directly for the next step without purification. $^1$H NMR (400 MHz, $CDCl_3$) $\delta$ 7.34-7.17 (m, 5H), 5.24-5.18 (m, 1H), 3.71 (d, $J_{AB}$ = 13.0 Hz, 1H), 3.64 (d, $J_{AB}$ = 13.0 Hz, 1H), 3.01 (s, 3H), 2.89-2.80 (m, 3H), 2.56-2.50 (m, 1H), 2.38-2.31 (m, 1H), 2.14 -2.07 (m, 1H).

**Synthesis of (*R*)-1-benzyl-3-cyanopyrrolidine (6)**

(*S*)-Methanesulfonic acid 1-benzyl-pyrrolidin-3-yl ester (28 g, 110 mmol) was dissolved in anhydrous acetonitrile (60 mL) and solid tetrabutylammonium cyanide (59 g, 220 mmol) was added at once at room temperature. The resulting mixture was heated at 65ºC for 16 h and cooled to room temperature. Saturated $NaHCO_3$ (100 mL) solution was added. The organic layer was then separated and the aqueous layer extracted with toluene (3x100 mL). The combined organic layers were washed with water (3x100 mL), brine, and dried over $Na_2SO_4$ and concentrated under reduced pressure to give (*R*)-1-benzyl-3-cyanopyrrolidine as brown oil (21 g), which was vacuum distilled at 150°C/5 mmHg to give a colorless liquid (19 g, 85%): $[\alpha]^{23}$ - 22.0º (c = 2.5, MeOH); $^1$H NMR (400 MHz, $CDCl_3$) $\delta$ 7.36-7.17 (m, 5H), 3.66 (*app* s, 2H), 3.05-2.99 (m, 1H), 2.93 (*app* t, *J* = 8.8 Hz, 1H), 2.72-2.60 (m, 3H), 2.31-2.22 (m, 1H), 2.17-2.11 (m, 1H).

**Synthesis of (*R*)-1-(1-Benzyl-pyrrolidin-3-yl)-cyclopropylamine (7)**

To a solution of (*R*)-1-benzyl-3-cyanopyrrolidine (**6,** 10 g, 53.4 mmol) in anhydrous ether (200 mL) was added $Ti(OiPr)_4$ (17.2 mL, 58.8 mmol) and the resulting solution was cooled to -78ºC. EtMgBr (3.0 M in $Et_2O$, 35 mL, 105 mmol, Aldrich) was added drop-wise during a period of 40

min at -78°C. Anhydrous THF (50 mL) was added to the resultant yellow suspension to facilitate stirring and the solution was stirred for 20 min at -78ºC. The reaction mixture was allowed slowly to warm up to room temperature, then $BF_3 \cdot Et_2O$ (13.4 mL, 107 mmol) was added and the resultant dark brown suspension was stirred at room temperature for 2 hrs. Both 1N HCl (100 mL) and $Et_2O$ (200 mL) were introduced subsequently to the reaction mixture and stirring was kept for 20 min until both organic and aqueous phases became clear. It was then basified using aqueous 20% NaOH (100 mL) and stirred for 30 min. The organic phase was separated and the aqueous phase was extracted with $Et_2O$ (2x100 mL). The combined organic phase was dried over $Na_2SO_4$ and concentrated under reduced pressure to give (*R*)-1-(1-benzyl-pyrrolidin-3-yl)-cyclopropylamine as brown oil (10.5 g, 90%), which was vacuum distilled to give a colorless liquid (9 g, 77%). The product is sufficiently pure to use in next step. For characterization, a small amount of sample was purified by PTLC using solvent $NH_4OH/MeOH/CH_2Cl_2$ (1/60/340): $[\alpha]^{23}$ - 10.0º (c = 2.5, MeOH); $^1$H NMR (400 MHz, $CDCl_3$) $\delta$ 7.33-7.23 (m, 5H), 3.62 (d, $J_{AB}$ = 12.8 Hz, 1H), 3.56 (d, $J_{AB}$ = 12.8 Hz, 1H), 2.66-2.57 (m, 3H), 2.40-2.37 (m, 1H), 1.96-1.91 (m, 2H), 1.69-1.62 (m, 1H), 0.55-0.48 (m, 2H), 0.41-0.36 (m, 2H).

**Synthesis of (R)-4-{[1-(1-Benzyl-pyrrolidin-3-yl)-cyclopropyl]-methyl-amino}-piperidine-1-carboxylic acid tert-butyl ester (9)**

To a solution of (R)-1-(1-benzyl-pyrrolidin-3-yl)-cyclopropylamine (**7,** 18.6 g, 87 mmol) and 4-oxo-piperidine-1-carboxylic acid tert-butyl ester (**8**, 22.7 g, 113 mmol) in THF (500 mL) was added glacial HOAc (31 mL). The solution was stirred at room temperature for one hour and then $NaBH(OAc)_3$ (65 g, 306 mmol) was added. The resulted suspension was stirred at room temperature overnight before 37% aqueous solution of formaldehyde (30 mL, 262 mmol) was added. The reaction mixture was allowed to stir for 3 hrs and completed, then added aqueous 20% NaOH (300 mL) at 0°C. The mixture was allowed to stir for 2 h, and layers were separated. The aqueous layer was extracted with EtOAc (3x300 mL). The combined organic phase was

dried over sodium sulfate, concentrated in vacuo. The residue was purified by flash chromatography (gradient elution, 1% to 10% methanol in dichloromethane) to give the title compound as a pale yellow oil (27 g): ESI MS m/z 414.3 ($M + H^+$). $^1$H NMR (400 MHz, $CDCl_3$) $\delta$ 7.33-7.23 (m, 5H), 4.24-4.02 (m, 2H), 3.88-3.80 (m, 1H), 3.60 (d, $J_{AB}$ = 12.8 Hz, 1H), 3.53 (d, $J_{AB}$ = 12.8 Hz, 1H), 2.82-2.57 (m, 5H), 2.31 (s, 3H), 2.28-2.22 (m, 1H), 1.94-1.80 (m, 4H), 1.44 (s, 9H), 1.42-1.28 (m, 3H), 0.55-0.53 (m, 4H). The chiral purity of the product was analyzed by Chiral-Cel OD column (0.46 cm × 25 cm, Daicel Chemical industries, Ltd, column catalog no. OD00CE-E1031) with acetonitrile in the presence of 0.1% diethylamine as mobile phase (flow rate 1mL/min; retention time 5.23 min desired, 5.93 isomer) to be 95% ee.

**Synthesis of (R)-4-[Methyl-(1-pyrrolidin-3-yl-cyclopropyl)-amino]-piperidine-1-carboxylic acid tert-butyl ester (10)**

(R)-4-{[1-(1-benzyl-pyrrolidin-3-yl)-cyclopropyl]-methyl-amino}-piperidine-1-carboxylic acid tert-butyl ester (**9,** 14 g) was dissolved in 150 mL glacial acetic acid at room temperature in a hydrogenation flask, air was evacuated, and filled with nitrogen. To this was added 30% Pd/C (5 g), flask was mounted to Parr shaker, nitrogen was evacuated and filled with hydrogen, and the mixture was shaken under hydrogen atmosphere at 60 psi in a Parr for 18 h. Reaction mixture was diluted with toluene (300 mL), filtered through a pad of celite. The filtrate was concentrated in vacuo, residue was digested in cold 30%NaOH at 0$^o$C and the product was extracted with ethyl acetate. The combined ethyl acetate solution was charged with 50 g of charcoal (Darco G-60), allowed to stir for 2 h, filtered, concentrated to give pale yellow oil, which can be vacuum distilled to give a clear oil (9.6 g). $^1$H NMR (400 MHz, $CD_3OD$) $\delta$ 4.04 (br s, 1H), 3.01 (dd, *J* = 10.4 Hz and 7.6 Hz, 1H), 2.84 (dd, *J* = 8.0 Hz and 5.2 Hz, 2H), 2.64-2.55 (m, 3H), 2.48-2.43 (m, 2H), 2.30 (s, 3H), 2.28-2.23 (m, 1H), 2.23-1.74 (m, 3H), 1.40 (s, 9H), 1.35-1.28 (m, 2H), 1.18-1.12 (m, 2H), 0.53-0.45 (m, 4H).

**Synthesis of 8-(3-{1-[(1-tert-Butoxycarbonyl-piperidin-4-yl)-methyl-amino]-cyclopropyl}-pyrrolidin-1-yl)-1-cyclopropyl-7-fluoro-9-methyl-4-oxo-4H-quinolizine-3-carboxylic acid ethyl ester (12)**

A stirred solution of ethyl 8-chloro-1-cyclopropyl-7-fluoro-9-methyl-4-oxo-4H-quinolizinone-3-carboxylate (**11,** 8.4 g, 25 mmol) and 4-[methyl-(1-pyrrolidin-3-yl-cyclopropyl)-amino]-piperidine-1-carboxylic acid tert-butyl ester (**10,** 10.6 g, 25 mmol) in the presence of sodium bicarbonate (8 g) in acetonitrile (150 mL) in a round bottom flask was heated under reflux for 5 hours. The solvent was removed *in vacuo*, residue was partitioned into 1N NaOH and ethyl acetate and well-shaken. The organic layer was separated, washed with brine, dried over sodium sulfate and concentrated in vacuo. The residue was purified by flash chromatography (75% ethyl acetate in hexane, then 10%MeOH in dichloromethane) to give a yellow solid (15 g, 99%). ESI MS *m/z* 611.3 ($M + H^+$). $^1$H NMR (400 MHz, $CDCl_3$) $\delta$ 9.25 (d, $J$ = 10.8 Hz, 1H), 8.18 (s, 1H), 4.42-4.37 (m, 2H), 4.15-4.10 (m, 3H), 3.92-3.88 (m, 1H), 3.58-3.56 (m, 2H), 3.48-3.44 (m, 1H), 2.73-2.62 (m, 5H), 2.57 (s, 3H), 2.39 (s, 3H), 2.18-2.13 (m, 1H), 2.00-1.94 (m, 1H), 1.84-1.78 (m, 2H), 1.46 (s, 9H), 1.42 (t, $J$ = 7.2 Hz, 3H), 1.28-1.25 (m, 1H), 1.07-0.93 (m, 2H), 0.84-0.68 (m, 4H), 0.60-0.52 (m, 2H).

**Synthesis of 1-Cyclopropyl-7-fluoro-9-methyl-8-{3-[1-(methyl-piperidin-4-yl-amino)-cyclopropyl]-pyrrolidin-1-yl}-4-oxo-4H-quinolizine-3-carboxylic acid (13)**

To a solution of 8-(3-{1-[(1-tert-butoxycarbonyl-piperidin-4-yl)-methyl-amino]-cyclopropyl}-pyrrolidin-1-yl)-1-cyclopropyl-7-fluoro-9-methyl-4-oxo-4H-quinolizine-3-carboxylic acid ethyl ester (**12,** 15 g, 24 mmol) in ethanol (200 mL) was added the solution of LiOH (10 g, 238 mmol) in water (100 mL) in a round bottom flask. The solution was heated at 60$^o$C for one hour. The resulting solution was partitioned between dichloromethane (400 mL) and saturated aqueous $NH_4Cl$ (200 mL) and well shaken. The organic layer was separated, washed with brine, dried

over sodium sulfate and concentrated in *vacuo* to yield a yellow solid (14 g). This was used without further purification. To a stirred solution of above compound (14 g) in dichloroethane (100 mL) was added trifluoroacetic acid (30 mL) at 0°C slowly. The resulting solution was stirred at 0°C to room temperature for one hour. The solvent was removed in vacuo to yield yellow oil, which was dissolved in 20% IPA in dichloromethane and the solution was neutralized by sat. aq $NaHCO_3$ resulting two clear phases, and the two phases were well shaken. The organic layer was separated, and the aqueous phase was extracted with 20% IPA/$CH_2Cl_2$. The combined organic extracts were washed with brine, dried over sodium sulfate and concentrated in *vacuo* to give yellow solid (10 g), the solid was crystallized from methanol/water to give crystalline solid (8 g). ESI MS *m/z* 483.3 ($M + H^+$). $^1H$ NMR (400 MHz, $CD_3OD$) $\delta$ 8.88 (d, $J$ = 10.0 Hz, 1H), 7.93 (s, 1H), 4.03-3.98 (m, 1H), 3.79-3.75 (m, 1H), 3.66-3.62 (m, 1H), 3.58-3.52(m, 1H), 3.47-3.44 (m, 2H), 3.05-2.88 (m, 4H), 2.62 (s, 3H), 2.49 (s, 3H), 2.35-2.23 (m, 3H), 2.06-2.02 (m, 1H), 1.70-1.58 (m, 2H), 1.51-1.44 (m, 1H), 0.93-0.64 (m, 8H).

**Synthesis of (*R*)-3-[(4-{1-[1-(3-Carboxy-1-cyclopropyl-7-fluoro-9-methyl-4-oxo-4*H*-quinolizine-8-yl)-pyrrolidin-3-yl-cyclopropyl]-methylamino}-piperidin-1-ylimino)-methylenyl]-rifamycin SV (1)**

1-Cyclopropyl-7-fluoro-9-methyl-8-{3-[1-(methyl-piperidin-4-yl-amino)-cyclopropyl]-pyrrolidin-1-yl}-4-oxo-4H-quinolizine-3-carboxylic acid (**13,** 9.2 g, 19 mmol) was dissolved in 1 N NaOH solution (120 mL) at room temperature. This was cooled to 0°C and under argon atmosphere. To this homogenous solution was added a freshly-prepared solution of hydroxylamine-*O*-sulfuric acid ($H_2N$-$OSO_3H$, 2 g, 18.5 mmol) in $H_2O$ (10 mL) dropwise at 0°C. The resultant solution was stirred at this temperature for 1 h, excess acetic acid (22 mL) was added to acidify to pH 5, followed by ascorbic acid (1 g). The solution was then diluted with methanol (280 mL). To the stirred resultant solution at room temperature, was added a homogeneous solution of 3-formylrifamycin (**14,** 8.2 g, 11.3 mmol in 40 mL of methanol/THF (3:1) slowly in 30 min. The

product slowly precipitates out of homogenous reaction mixture. After addition, the stirred reaction mixture was kept for 30 min at room temperature and cooled to 0 $^{o}$C for 1 h, and precipitate was collected, and washed with cold methanol (3x20 mL) to give 9.5 g. The collected precipitate was dissolved in dichloromethane (100 mL), this solution was stirred with 5% citric acid solution (100 mL) in the presence of 0.5% ascorbic acid for two hours and the two phases were shaken. Organic phase was separated, washed with the same aqueous solution, dried over sodium sulfate. To the dried filtrate, added half the volume of ethanol and concentrated in vacuo to give an orange solid (8.5 g). One gram of the orange solid was crystallized as follows: The solid (1 gram) was dissolved in 5 mL of acetone and water (95:5), the stirred solution was heated on an oil-bath at 55-60 $^{o}$C until homogeneous. The solution was slowly cooled with stirring (200 rpm) to room temperature. Once precipitate forms, the mixture was allowed to stir at room temperature for 2 h, and cooled to 0$^{o}$C on ice-bath for 2 h, before collecting the precipitate using a Buchner funnel with aid of cold solvent. The cake was pressed-dry, and washed with 5 mL cold acetone/water (95:5) and pressed-dry again. The cake was vacuum dried to a constant weight (830 mg obtained) to produce the title compound. $^{1}$H NMR (400 MHz, $CDCl_3$) $\delta$ 13.82 (s, 1H), 13.52 (*br* s, 1 H), 13.25 (singlet, 1H), 11.98 (singlet, 1H), 9.04 (d, *J* = 9.2 Hz, 1H), 8.22 (s 1H), 7.97 (s, 1H), 6.58-6.50 (m, 1H), 6.37-6.34 (m, 1H), 6.18 (d, *J* = 12.4 Hz, 1H), 5.94-5.87 (m, 1H), 5.07 (dd, *J* = 6.8, 12.8 Hz, 1H), 4.89 (d, *J* = 10.8 Hz, 1H), 3.93-3.87 (m, 1H), 3.72 (d, *J* = 9.6 Hz, 1H), 3.66-3.52 (m, 4H), 3.48-3.42 (m, 3H), 3.00 (s, 3H), 3.00-2.95 (m, 1H), 2.65-2.50 (m, 6H), 2.37 (s, 3H), 2.36-2.30 (m, 1H), 2.19 (s, 3H), 2.18-2.10 (m, 1H), 2.02 (*app* s, 6H), 2.00-1.82 (m, 2H), 1.76 (s, 3H), 1.65-1.40 (m, ~10H), 1.32-1.17 (m, 2H), 1.08-1.02 (m, 1H), 0.96 (d, *J* = 6.8 Hz, 3H), 0.90-0.85 (m, 1H), 0.82 (d, *J* = 6.8 Hz, 3H), 0.78-0.62 (m, 3H), 0.56 (d, *J* = 6.4 Hz, 3H), -0.35 (d, *J* = 6.8 Hz, 3H); MS: ESI *m/z* 1173.6 (M –MeO, most abundant)$^{+}$, 1205.6 (M + H, parent)$^{+}$; HPLC purity: 98.9%.

## ASSOCIATED CONTENT

## Supporting Information

Molecular formula strings and biochemical activity data (CSV).

## AUTHOR INFORMATION

### Corresponding author

*Phone: +86 512-8686-1980, Fax: +86 512-8686-1986, E-mail: zhenkun.ma@tennorx.com.

### Notes

The authors declare the following competing financial interest(s): Ma and Lynch were both employees of Cumbre Pharmaceuticals where dual-acting compound **1** was discovered. Ma is a founder and employee of TenNor Therapeutics currently developing compound **1**.

## ACKNOWLEDGEMENTS

The work reviewed in this article represents many years of effort by a large number of distinguished colleagues, first at Cumbre Pharmaceuticals and now continued at TenNor Therapeutics. Their tremendous contribution to the discovery and development of dual-acting antimicrobial series is greatly appreciated.

## ABBREVIATIONS USED

ADME, absorption, distribution, metabolism and excretion; ATCC, American Type Culture Collection; CFU, colony forming unit; CoNS, coagulase-negative staphylococci; cSSSI, complicated skin and skin structure infection; CVC, central venous catheter; CYP, cytochrome P450; FIC, fractional inhibitory concentration; FQ, fluoroquinolone; hERG, human Ether-a-go-go Related Gene; IDSA, Infectious Diseases Society of America; IE, infective endocarditis; MBC, minimum bactericidal concentration; MIC, minimum inhibitory concentration; MPC, mutation

prevention concentration; MRSA, methicillin-resistant *Staphylococcus aureus*; MSSA, methicillin-sensitive *Staphylococcus aureus*; PJI, prosthetic joint infection; QMRSA, quinolone-resistant, methicillin-resistant *Staphylococcus aureus*; RNAP, RNA polymerase.

## REFERENCES

1. Kapadia, B. H.; Berg, R. A.; Daley, J. A.; Fritz, J.; Bhave, A.; Mont, M. A., Periprosthetic joint infection. *J. Lancet* **2015,** *387* (10016), 386-394.

2. Tande, A. J.; Patel, R., Prosthetic joint infection. *Clin. Microbiol. Rev.Clin. Microbiol. Rev.Clin. Microbiol. Rev.* **2014,** *27* (2), 302-345.

3. Osmon, D. R.; Berbari, E. F.; Berendt, A. R.; Lew, D.; Zimmerli, W.; Steckelberg, J. M.; Rao, N.; Hanssen, A.; Wilson, W. R., Executive summary: Diagnosis and management of prosthetic joint infection: Clinical practice guidelines by the Infectious Diseases Society of America. *Clin. Infect. Dis.* **2013,** *56* (1), 1-10.

4. (a) McConoughey, S. J.; Howlin, R.; Granger, J. F.; Manring, M. M.; Calhoun, J. H.; Shirtliff, M.; Kathju, S.; Stoodley, P., Biofilms in periprosthetic orthopedic infections. *Future Microbiol.* **2014,** *9* (8), 987-1007; (b) Gbejuade, H. O.; Lovering, A. M.; Webb, J. C., The role of microbial biofilms in prosthetic joint infections. *Acta Orthop.* **2015,** *86* (2), 147-158.

5. Ma, Z.; Morris, T. W.; Combrink, K. D., Therapeutic opportunities for the treatment of biofilm-associated infections. In *Annu. Rep. Med. Chem.Annu. Rep. Med. Chem.*, Academic Press: 2004; Vol. Volume 39, pp 197-210.

6. (a) Trampuz, A.; Zimmerli, W., Diagnosis and treatment of implant-associated septic arthritis and osteomyelitis. *Current infectious disease reports* **2008,** *10* (5), 394-403; (b) Sendi, P.; Zimmerli, W., Antimicrobial treatment concepts for orthopaedic device-related infection. *Clin. Microbiol. Infect.* **2012,** *18* (12), 1176-1184; (c) Holmberg, A.; Thórhallsdóttir, V. G.; Robertsson, O.; W-Dahl, A.; Stefánsdóttir, A., 75% success rate after open debridement, exchange of tibial insert, and antibiotics in knee prosthetic joint infections. *Acta Orthop.* **2015,** *86* (4), 457-462.

7. Sensi, P., History of the development of rifampin. *Rev. Infect. Dis.* **1983,** *5 Suppl 3*, S402-406.

8. Ma, Z.; Ginsberg, A. M.; Spigelman, M., 7.24 - Antimycobacterium agents. In *Compr. Med. Chem. II II*, Triggle, J. B. T. J., Ed. Elsevier: Oxford, 2007; pp 699-730.

9. DuPont, H. L., Therapeutic effects and mechanisms of action of rifaximin in gastrointestinal diseases. *Mayo Clin. Proc.* **2015,** *90* (8), 1116-1124.

10. Campbell, E. A.; Korzheva, N.; Mustaev, A.; Murakami, K.; Nair, S.; Goldfarb, A.; Darst, S. A., Structural mechanism for rifampicin inhibition of bacterial RNA polymerase. *Cell* **2001,** *104* (6), 901-912.

11. (a) Goldstein, B. P., Resistance to rifampicin: a review. *J Antibiot* **2014,** *67* (9), 625-630; (b) Mariam, D. H.; Mengistu, Y.; Hoffner, S. E.; Andersson, D. I., Effect of rpoB mutations conferring rifampin resistance on fitness of Mycobacterium tuberculosis. *Antimicrob. Agents Chemother.* **2004,** *48* (4), 1289-1294.

12. Koch, A.; Mizrahi, V.; Warner, D. F., The impact of drug resistance on Mycobacterium tuberculosis physiology: what can we learn from rifampicin? *Emerging Microbes Infect.* **2014,** *3* (3), e17.

13. (a) Al-Omari, A.; Cameron, D. W.; Lee, C.; Corrales-Medina, V. F., Oral antibiotic therapy for the treatment of infective endocarditis: a systematic review. *BMC Infect. Dis.* **2014,** *14*, 140. doi:10.1186/1471-2334-14-140; (b) Coiffier, G.; Albert, J.-D.; Arvieux, C.; Guggenbuhl, P., Optimizing combination rifampin therapy for staphylococcal osteoarticular infections. *Jt., Bone, Spine* **2013,** *80* (1), 11-17; (c) Forrest, G. N.; Tamura, K., Rifampin combination therapy for nonmycobacterial infections. *Clin Microbiol Rev* **2010,** *23* (1), 14-34.

14. (a) Sanchez, C. J., Jr.; Shiels, S. M.; Tennent, D. J.; Hardy, S. K.; Murray, C. K.; Wenke, J. C., Rifamycin derivatives are effective against staphylococcal biofilms in vitro and elutable from PMMA. *Clin. Orthop. Relat. Res.* **2015,** *473* (9), 2874-2884; (b) Hall Snyder, A. D.; Vidaillac, C.; Rose, W.; McRoberts, J. P.; Rybak, M. J., Evaluation of high-dose daptomycin versus

vancomycin alone or combined with clarithromycin or rifampin against Staphylococcus aureus and S. epidermidis in a novel in vitro PK/PD model of bacterial biofilm. *Infect. Dis. Ther.* **2015**; 4(1): 51–65; (c) Mihailescu, R.; Furustrand Tafin, U.; Corvec, S.; Oliva, A.; Betrisey, B.; Borens, O.; Trampuz, A., High activity of fosfomycin and rifampin against methicillin-resistant staphylococcus aureus biofilm in vitro and in an experimental foreign-body infection model. *Antimicrob. Agents Chemother.* **2014,** *58* (5), 2547-2553.

15. Minassian, A. M.; Osmon, D. R.; Berendt, A. R., Clinical guidelines in the management of prosthetic joint infection. *J. Antimicrob. Chemother.* **2014,** *69 Suppl 1*, i29-35.

16. (a) Widmer, A. F.; Gaechter, A.; Ochsner, P. E.; Zimmerli, W., Antimicrobial treatment of orthopedic implant-related infections with rifampin combinations. *Clin. Infect. Dis.* **1992,** *14* (6), 1251-1253; (b) Zimmerli, W.; Widmer, A. F.; Blatter, M.; Frei, R. R.; Ochsner, P. E.; Role of rifampin for treatment of orthopedic implant–related staphylococcal infections : A randomized controlled trial. Foreign-Body Infection (FBI) Study Group. *JAMA* **1998,** *279* (19), 1537-1541; (c) Trampuz, A.; Zimmerli, W., Antimicrobial agents in orthopaedic surgery: Prophylaxis and treatment. *Drugs* **2006,** *66* (8), 1089-1105.

17. Tang, H.-J.; Lai, C.-C.; Hsueh, P.-R.; Chen, C.-C.; Wu, K.-Y.; Lin, Y.-C.; Zhang, C.-C.; Weng, T.-C.; Chiu, Y.-H.; Toh, H.-S.; Chiang, S.-R.; Yu, W.-L.; Ko, W.-C.; Chuang, Y.-C., RNA polymerase B subunit gene mutations in biofilm-embedded methicillin-resistant Staphylococcus aureus following rifampin treatment. *J. Microbiol., Immunol. Infect.* **2015**, 48 (4), 400-408.

18. (a) Bahl, D.; Miller, D. A.; Leviton, I.; Gialanella, P.; Wolin, M. J.; Liu, W.; Perkins, R.; Miller, M. H., In vitro activities of ciprofloxacin and rifampin alone and in combination against growing and nongrowing strains of methicillin-susceptible and methicillin-resistant Staphylococcus aureus. *Antimicrob. Agents Chemother.* **1997,** *41* (6), 1293-1297; (b) Murillo, O.; Pachon, M. E.; Euba, G.; Verdaguer, R.; Tubau, F.; Cabellos, C.; Cabo, J.; Gudiol, F.; Ariza, J., Antagonistic effect of rifampin on the efficacy of high-dose levofloxacin in staphylococcal experimental foreign-body infection. *Antimicrob. Agents Chemother.* **2008,** *52* (10), 3681-3686;

(c) Balasubramanian, V.; Solapure, S.; Gaonkar, S.; Mahesh Kumar, K. N.; Shandil, R. K.; Deshpande, A.; Kumar, N.; Vishwas, K. G.; Panduga, V.; Reddy, J.; Ganguly, S.; Louie, A.; Drusano, G. L., Effect of coadministration of moxifloxacin and rifampin on Mycobacterium tuberculosis in a murine aerosol infection model. *Antimicrob. Agents Chemother.* **2012,** *56* (6), 3054-3057.

19. (a) Bremner, J. B.; Ambrus, J. I.; Samosorn, S., Dual action-based approaches to antibacterial agents. *Curr. Med. Chem.* **2007,** *14* (13), 1459-1477; (b) Pokrovskaya, V.; Baasov, T., Dual-acting hybrid antibiotics: a promising strategy to combat bacterial resistance. *Expert Opin. Drug Discovery* **2010,** *5* (9), 883-902; (c) Tevyashova, A. N.; Olsufyeva, E. N.; Preobrazhenskaya, M. N., Design of dual action antibiotics as an approach to search for new promising drugs. *Russ. Chem. Rev.* **2015,** *84* (1), 61-97; (d) Barbachyn, M. R., Chapter 17 - Recent advances in the discovery of hybrid antibacterial agents. In *Annu. Rep. Med. Chem.*, John, E. M., Ed. Academic Press: 2008; Vol. Volume 43, pp 281-290.

20. (a) Georgopapadakou, N. H.; Bertasso, A.; Chan, K. K.; Chapman, J. S.; Cleeland, R.; Cummings, L. M.; Dix, B. A.; Keith, D. D., Mode of action of the dual-action cephalosporin Ro 23-9424. *Antimicrob. Agents Chemother.* **1989,** *33* (7), 1067-1071; (b) Christenson, J. G.; Chan, K. K.; Cleeland, R.; Dix-Holzknecht, B.; Farrish, H. H., Jr.; Patel, I. H.; Specian, A., Pharmacokinetics of Ro 23-9424, a dual-action cephalosporin, in animals. *Antimicrob. Agents Chemother.* **1990,** *34* (10), 1895-1900.

21. Gu, J. W.; Neu, H. C., In vitro activity of Ro 23-9424, a dual-action cephalosporin, compared with activities of other antibiotics. *Antimicrob. Agents Chemother.* **1990,** *34* (2), 189-195.

22. Locher, H. H.; Caspers, P.; Bruyere, T.; Schroeder, S.; Pfaff, P.; Knezevic, A.; Keck, W.; Ritz, D., Investigations of the mode of action and resistance development of cadazolid, a new antibiotic for treatment of Clostridium difficile infections. *Antimicrob. Agents Chemother.* **2014,** *58* (2), 901-908.

23. Ding, C. Z.; Ma, Z.; Li, J.; Harran, S.; He, Y.; Minor, K. P.; Kim, I. H.; Longgood, J. C.; Jin, Y.; Combrink, K. D., (R/S) rifamycin derivatives, their preparations and pharmaceutical compositions. US Patent 7,226,931 (**2007**).

24. (a) Kim, I. H.; Combrink, K. D.; Ma, Z.; Chapo, K.; Yan, D.; Renick, P.; Morris, T. W.; Pulse, M.; Simecka, J. W.; Ding, C. Z., Synthesis and antibacterial evaluation of a novel series of rifabutin-like spirorifamycins. *Bioorg. Med. Chem. Lett.* **2007,** *17* (5), 1181-1184; (b) Ma, Z.; Kim, I. H.; Li, J., Spiro-rifamycin derivatives targeting RNA polymerase. US Patent 7,202,246 (**2007**); (c) Ding, C. Z.; Kim, I. H.; Wang, J.; Ma, Z.; Jin, Y.; Combrink, K. D.; Lu, G.; Lynch, A. S., Nitroheteroaryl-containing rifamycin derivatives. US Patent 7,678,791 (**2010**).

25. (a) Li, J.; Ma, Z.; Chapo, K.; Yan, D.; Lynch, A. S.; Ding, C. Z., Preparation and in vitro anti-staphylococcal activity of novel 11-deoxy-11-hydroxyiminorifamycins. *Bioorg. Med. Chem. Lett.* **2007,** *17* (20), 5510-5513; (b) Li, J.; Ding, C. Z.; Ma, Z., Rifamycin C-11 oxime derivatives effective against drug-resistant microbes. US Patent 7,265,107 (**2007**); (c) Li, J.; Ma, Z., Rifamycin C-11 oxime cyclo derivatives effective against drug-resistant microbes. US Patent 7,256,187 (**2007**).

26. (a) Combrink, K. D.; Denton, D. A.; Harran, S.; Ma, Z.; Chapo, K.; Yan, D.; Bonventre, E.; Roche, E. D.; Doyle, T. B.; Robertson, G. T.; Lynch, A. S., New C25 carbamate rifamycin derivatives are resistant to inactivation by ADP-ribosyl transferases. *Bioorg. Med. Chem. Lett.* **2007,** *17* (2), 522-526; (b) Combrink, K.; Harran, S.; Denton, D.; Ma, Z., C-25 carbamate rifamycin derivatives with activity against drug-resistant microbes. US Patent 7,250,413 (**2007**).

27. Ding, C. Z.; Jin, Y.; Combrink, K.; Kim, I. H., Quinolone carboxylic acid-substituted rifamycin derivatives. US Patent 7,884,099 (**2011**).

28. Ma, Z.; Jin, Y.; Li, J.; Ding, C. Z.; Minor, K. P.; Longgood, J. C.; Kim, I. H.; Harran, S.; Combrink, K.; Morris, T. W., Rifamycin derivatives effective against drug-resistant microbes. US Patent 7,247,634 (**2007**).

29. Li, Q.; Mitscher, L. A.; Shen, L. L., The 2-pyridone antibacterial agents: bacterial topoisomerase inhibitors. *Med. Res. Rev.* **2000,** *20* (4), 231-293.

30. (a) Saiki, A. Y.; Shen, L. L.; Chen, C. M.; Baranowski, J.; Lerner, C. G., DNA cleavage activities of Staphylococcus aureus gyrase and topoisomerase IV stimulated by quinolones and 2-pyridones. *Antimicrob. Agents Chemother.* **1999,** *43* (7), 1574-1577; (b) Meulbroek, J. A.; Oleksijew, A.; Tanaka, S. K.; Alder, J. D., Efficacy of ABT-719, a 2-pyridone antimicrobial, against enterococci, Escherichia coli, and Pseudomonas aeruginosa in experimental murine pyelonephritis. *J. Antimicrob. Chemother.* **1996,** *38* (4), 641-653.

31. (a) Robertson, G. T.; Bonventre, E. J.; Doyle, T. B.; Du, Q.; Duncan, L.; Morris, T. W.; Roche, E. D.; Yan, D.; Lynch, A. S., In vitro evaluation of CBR-2092, a novel rifamycin-quinolone hybrid antibiotic: studies of the mode of action in Staphylococcus aureus. *Antimicrob. Agents Chemother.* **2008,** *52* (7), 2313-2323; (b) Robertson, G. T.; Bonventre, E. J.; Doyle, T. B.; Du, Q.; Duncan, L.; Morris, T. W.; Roche, E. D.; Yan, D.; Lynch, A. S., In vitro evaluation of CBR-2092, a novel rifamycin-quinolone hybrid antibiotic: microbiology profiling studies with staphylococci and streptococci. *Antimicrob. Agents Chemother.* **2008,** *52* (7), 2324-2334.

32. (a) Lynch, A. S.; Bonventre, E. J.; Doyle, T. B.; Du, Q.; DUNCAN, L.; Robertson, G. T.; Roche, E. D., *In vitro* mode-of-action studies of CBR-2092: a novel rifamycin-quinolone hybrid antibiotic. *ICAAC Poster* **2007,** *F1-2101*; (b) Robertson, G. T.; Bonventre, E. J.; Doyle, T. B.; Du, Q.; Duncan, L.; Roche, E. D.; Lynch, A. S., Comparative *in vitro* activity of CBR-2092, a novel rifamycin-quinolone hybrid antibiotic, and rifampin+quinolone combinations. *ICAAC Poster* **2007,** *F1-2102*; (c) Du, Q.; Doyle, T. B.; Duncan, L.; Robertson, G. T.; Lynch, A. S., *In vitro* microbiology profiling of CBR-2092, a novel rifamycin-quinolone hybrid antibiotic. *ICAAC Poster* **2007,** *F1-2103*; (d) Doyle, T. B.; Bonventre, E. J.; Du, Q.; Robertson, G. T.; Roche, E. D.; Lynch, A. S., *In vitro* studies of the efficacy of CBR-2092, a novel rifamycin-quinolone hybrid antibiotic, in killing staphylococcal cells in biofilms. *ICAAC Poster* **2007,** *F1-2104*; (e) Renick, P. J.; Morris, T. W.; Nguyen, P. M.; Pulse, M. E.; Weiss, W. J., Efficacy of CBR-2092, a novel rifamycin-

quinolone yybrid antibiotic, in rodent models of bacterial infection. *ICAAC Poster* **2007,** *F1-2105*; (f) Weiss, W. J.; Bao, D.; Miller, G. A.; Morris, T. W.; Nguyen, P. M.; Pulse, M. E.; Renick, P. J.; Truong, T., Pharmacokinetic and pharmacodynamic studies with CBR-2092, a novel rifamycin-quinolone hybrid antibiotic. *ICAAC Poster* **2007,** *F1-2106*; (g) Xiong, Y. Q.; Weiss, W. J.; Doyle, T. B.; Abdelsayed, G. A.; Bayer, A. S., Efficacy of CBR-2092, a novel rifamycin-quinolone hybrid antibiotic, and vancomycin in experimental methicillin-resistant Staphylococcus aureus infective endocarditis. *ICAAC Poster* **2007,** *F1-2107*; (h) Xiong, Y. Q.; Weiss, W. J.; Doyle, T. B.; Abdelsayed, G. A.; Bayer, A. S., Comparative efficacy of CBR-2092 and conventional rifampin+quinolone combinations in experimental infective endocarditis caused by a quinolone-resistant MRSA. *ICAAC Poster* **2007,** *F1-2108*.

## TABLE OF CONTENTS GRAPHIC